

## PHONON DISPERSION IN CHIRAL SINGLE-WALL CARBON NANOTUBES

WEIHUA MU<sup>\*,†,§</sup>, ANTHONY NICKOLAS VAMIVAKAS<sup>‡</sup>,  
YAN FANG<sup>†</sup> and BOLIN WANG<sup>\*,†</sup>

<sup>\*</sup>*Institute of Theoretical Physics, The Chinese Academy of Sciences,  
P.O. Box 2735, Beijing 100080, China*

<sup>†</sup>*Beijing Key Lab for Nano-Photonics and Nano-Structure,  
Capital Normal University, Beijing 100037, China*

<sup>‡</sup>*Department of Electrical and Computer Engineering,  
Boston University, 8 St. Mary's Street, Boston, MA 02215, USA*

<sup>§</sup>*muwh@itp.ac.cn*

Received 24 April 2007

The method to obtain phonon dispersion of achiral single-wall carbon nanotubes (SWNTs) from  $6 \times 6$  matrix proposed by Mahan and Jeon<sup>7</sup> has been extended to chiral SWNTs. The number of calculated phonon modes of a chiral SWNT (10, 1) is much larger than that of a zigzag one (10, 0) because the number of atoms in the translational unit cell of chiral SWNT is larger than that of an achiral one even though they have relative similar radius. The possible application of our approach to other models with more phonon potential terms beyond Mahan and Jeon's model is discussed.

*Keywords:* Phonon; single-wall carbon nanotubes; chiral.

Single-wall carbon nanotube (SWNT) can be thought of as a sheet of graphite rolled into a seamless cylinder.<sup>1</sup> SWNTs have attracted much interest on their transport properties of heat or electricity. In electric transport process, scattering of the electrons by the phonons is of great importance.<sup>2</sup> Therefore SWNTs' phonon dispersions over the full Brillouin zone are necessary for computation of this topic. Theoretically, a number of approaches have been developed.<sup>3–18</sup> Ye *et al.*<sup>3</sup> used the *ab initio* supercell approach to obtain the phonon dispersion curves for chiral SWNTs. Their result is accurate only for the high-energy vibrations. Dubay and Kresse<sup>10</sup> used the full *ab initio* approach and zone folding method with the force constants obtained from the *ab initio* calculation to study the phonon dispersion relations of armchair and zigzag SWNTs, i.e., only achiral SWNTs. Mahan and Jeon<sup>7,19</sup> have pointed out the weakness of the zone folding method. The zone folding approach, which although works well for electric states, does not work for phonon states. Electron states are solutions to a scalar wave equation while phonon states are solutions to a vector wave equation. By *ab initio* calculations, Sánchez-Portal *et al.*<sup>9</sup> studied dispersion relations of SWNTs with different chiralities and radii. The

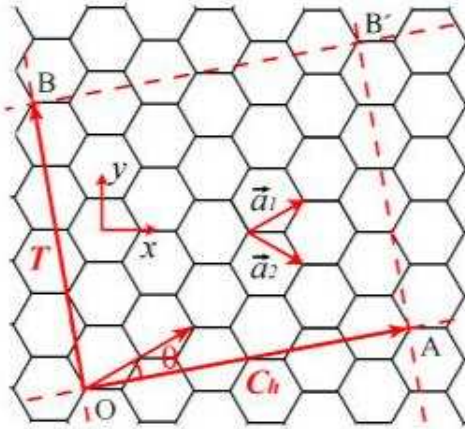


Fig. 1. The 2D sketch map of single-wall carbon nanotubes. This image was made with VMD and is owned by the Theoretical and Computational Biophysics Group, an NIH Resource for Macromolecular Modeling and Bioinformatics, at the Beckman Institute, University of Illinois at Urbana-Champaign.

system they studied involves approximate 100 carbon atoms, and needs large computer resources. Popov *et al.*<sup>4,6</sup> proposed a symmetry-adapted lattice-dynamical model for SWNTs. They considered the screw symmetry of the SWNT, kept a two-atom unit cell, and reduced the dynamical matrix to a six-by-six matrix for the SWNT with arbitrary chirality. They found that the breathing mode frequency is inversely proportional to the radius of the tube. Popov *et al.*'s work is one of the methods which transfer force constants from graphite to the SWNTs. However, their method needs many force constants determined by experiment. Mahan and Jeon proposed a model with minimal number of force constants to calculate the phonon dispersion of armchair and zigzag SWNTs,<sup>7</sup> obtained the physical results, but their approach is restricted to achiral SWNTs with highly symmetric structures.

In the present paper, we investigate theoretically the phonon dispersion of SWNTs with arbitrary chiral index  $(n, m)$ . We follow the algorithm proposed in Ref. 7 and extend it for our calculations to chiral SWNTs.

In SWNTs, we locate  $A$  atoms at the lattice site  $\mathbf{R}_j$  and their three nearest neighbors  $B$  atoms at site  $\mathbf{R}_j + \boldsymbol{\delta}$ . Unit vector  $\hat{\boldsymbol{\delta}}$  reflects the direction of  $\boldsymbol{\delta}$ . Figure 1 shows a commonly-used coordinate system for two-dimensional graphene, with primitive lattice vectors are  $\mathbf{a}_1 = \sqrt{3}a(\sqrt{3}/2, 1/2)$ ,  $\mathbf{a}_2 = \sqrt{3}a(\sqrt{3}/2, -1/2)$ . For SWNTs, the chiral vector is defined as  $\mathbf{C}_h = n\mathbf{a}_1 + m\mathbf{a}_2$ , the pair of integers  $(n, m)$  characterize the chirality of SWNT. When a sheet of graphite is rolled into a cylinder, the points  $(0, 0)$  and  $(n, m)$  coincide. The radius of SWNTs,  $R = |\mathbf{C}_h|/2\pi$ .

Consider a type  $A$  atom located at lattice site  $(t, l)$  on 2D graphite sheet. When the graphite layer rolls up to a  $(n, m)$  SWNT with radius  $R$ , the atom positions, in 3D Descartes coordinate system are  $(c = 3a/2, \theta_z = \sqrt{3}a/R)$

$$R_A = [R \cos(\theta_{tl}), R \sin(\theta_{tl}), \bar{l}c], \tag{1}$$

$$R_B^{(i)} = [R \cos(\theta_{tl} + u_i \theta_z), R \sin(\theta_{tl} + u_i \theta_z), \bar{l}c + av_i], \tag{2}$$

where

$$u_i = \begin{cases} \frac{n+m}{2\sqrt{n^2+nm+m^2}}, & i=1, \\ \frac{-n}{2\sqrt{n^2+nm+m^2}}, & i=2, \\ \frac{-m}{2\sqrt{n^2+nm+m^2}}, & i=3, \end{cases} \tag{3}$$

and

$$v_i = \begin{cases} \frac{n-m}{2\sqrt{n^2+nm+m^2}}, & i=1, \\ \frac{n+2m}{2\sqrt{n^2+nm+m^2}}, & i=2, \\ -\frac{2n+m}{2\sqrt{n^2+nm+m^2}}, & i=3, \end{cases} \tag{4}$$

with  $\bar{l} = \frac{\sqrt{3}}{2} \cdot \frac{ln-tm}{\sqrt{n^2+nm+m^2}}$  denoting the position along the  $z$ -axis. When  $m = n$  or  $0$ , our general expressions are reduced to those in Refs. 7 and 19.

In this notation, the three unit vectors  $\hat{\delta}_i$  are

$$\hat{\delta}^{(i)} = \left[ -\sqrt{3}u_i \sin\left(\theta_{tl} + \frac{u_i}{2}\theta_z\right), \sqrt{3}u_i \cos\left(\theta_{tl} + \frac{u_i}{2}\theta_z\right), v_i \right], \quad i = 1, 2, 3. \tag{5}$$

We keep a two-atom primal cell for SWNTs, however, different from Refs. 4 and 6, we exploit the screw symmetry of SWNTs in a cylindrical coordinate system, which is much easier to understand. For SWNTs, the basis of lattice vectors in real space are  $\alpha_1 = (\frac{2\pi}{N}, \tau) \equiv (\psi, \tau)$ ,  $\alpha_2 = (0, T)$ . The reciprocal lattice vectors are  $\beta_1 = (N, 0)$ ,  $\beta_2 = (-\frac{\tau N}{T}, \frac{2\pi}{T})$ .<sup>1,20</sup> Here,  $N = \frac{2(n^2+nm+m^2)}{d_R}$ ,  $T = \frac{3a\sqrt{n^2+nm+m^2}}{d_R}$ , and  $d_R$  is the greatest common divisor of  $2n+m$  and  $n+2m$ . Obviously,  $\alpha_i \cdot \beta_j = 2\pi\delta_{ij}$ ,  $i, j = 1, 2$ . For SWNTs, the phonon states have two quantum numbers  $(q, \alpha)$  to describe their wave vectors. In the first Brillouin zone,  $\alpha = 0, 1, \dots, N-1$ ,  $-\frac{\pi}{T} \leq qa \leq \frac{\pi}{T}$ .

In a cylindrical coordinate system  $[\rho, \theta, z]$ , the displacement of the atoms  $A$  and  $B$  in radial, tangential, and  $z$  directions are denoted by  $Q_{s\rho}, Q_{s\theta}, Q_{sz}$ , ( $s = A, B$ ),

so the displacement of atoms are

$$\begin{aligned}
 Q_{A,tl} &= Q_{A,tl,\rho}[\cos(\theta_{tl}), \sin(\theta_{tl}), 0] \\
 &\quad + Q_{A,tl,\theta}[-\sin(\theta_{tl}), \cos(\theta_{tl}), 0] + Q_{A,tl,z}[0, 0, 1],
 \end{aligned}
 \tag{6}$$

$$\begin{aligned}
 Q_{B,tl}^{(i)} &= Q_{B,tl,\rho}[\cos(\theta_{tl} + u_i\theta_z), \sin(\theta_{tl} + u_i\theta_z), 0] \\
 &\quad + Q_{B,tl,\theta}[-\sin(\theta_{tl} + u_i\theta_z), \cos(\theta_{tl} + u_i\theta_z), 0] \\
 &\quad + Q_{B,tl,z}[0, 0, 1], \quad i = 1, 2, 3.
 \end{aligned}
 \tag{7}$$

Introduce collective displacements  $Q_{A(B),q\alpha,r}$ ,

$$\begin{aligned}
 Q_{A,tl,r} &= \frac{1}{\sqrt{N}} \sum_{q\alpha} Q_{A,q\alpha,r} \exp[i(qc\bar{l}) + \alpha\theta_{tl}], \\
 Q_{B,tl,r}^{(i)} &= \frac{1}{\sqrt{N}} \sum_{q\alpha} Q_{B,q\alpha,r} \exp[i(qc\bar{l} + iqav_i) + \alpha(\theta_{tl} + u_i\theta_z)],
 \end{aligned}$$

where  $r = (\rho, \theta, z)$ . Since the displacement  $Q_{A(B),tl,r}$  is real, we have

$$Q_{A(B),q\alpha,r}^* = Q_{A(B),-q,-\alpha,r}
 \tag{8}$$

The phonon dispersion is found from a model with three adjustable force constants,<sup>7</sup> which is a spring and mass model with minimal number of parameters that give a physical result. The phonon potentials of this model reflect effects of first neighbor springs, second neighbor springs, and radial bond bending force. The phonon energies will vanish if the SWNT is rigidly translated or rigidly rotated along the axis. Therefore, the dynamical matrix obtained from these phonon potentials have correct symmetry, which ensures the phonon eigenvectors to be correct for the SWNTs.<sup>5,7,8</sup>

For the first neighboring spring, the phonon potential energy  $V_1$  is

$$V_1 = \frac{K_1}{2} \sum_{tl} \sum_{i=1}^3 |\Xi^{(i)}|^2,
 \tag{9}$$

$$\begin{aligned}
 \Xi^{(i)} &= \hat{\delta}_i \cdot (\mathbf{Q}_B^{(i)} - \mathbf{Q}_A) \\
 &= e^{i(qc\bar{l} + \beta\theta_{tl})} \tilde{\Xi}^{(i)}, \quad i = 1, 2, 3
 \end{aligned}
 \tag{10}$$

$$\begin{aligned}
 \tilde{\Xi}^{(i)} &= e^{iqav_i + i\alpha u_i\theta_z} \left( \sqrt{3}u_i \sin\left(\frac{u_i\theta_z}{2}\right) Q_{B,\rho} + \sqrt{3}u_i \cos\left(\frac{u_i\theta_z}{2}\right) Q_{B\theta} + v_i Q_{Bz} \right) \\
 &\quad + \sqrt{3}u_i \sin\left(\frac{u_i\theta_z}{2}\right) Q_{A\rho} - \sqrt{3}u_i \cos\left(\frac{u_i\theta_z}{2}\right) Q_{A\theta} - v_i Q_{Az}, \quad i = 1, 2, 3.
 \end{aligned}
 \tag{11}$$

The displacement  $Q$  is a complex quantity, the real and imaginary parts of which are independent variables, but we only need the force on  $Q$ ,  $\delta V/\delta Q^*$ , to obtain the

determinant equation

$$0 = \det \begin{pmatrix} M_{11} - \Omega_1^2 & M_{12} & M_{13} & M_{14} & M_{15} & M_{16} \\ (M_{12})^* & M_{22} - \Omega_1^2 & M_{23} & M_{24} & M_{25} & M_{26} \\ (M_{13})^* & (M_{23})^* & M_{33} - \Omega_1^2 & M_{34} & M_{35} & M_{36} \\ (M_{14})^* & (M_{24})^* & (M_{34})^* & M_{44} - \Omega_1^2 & M_{45} & M_{46} \\ (M_{15})^* & (M_{25})^* & (M_{35})^* & (M_{45})^* & M_{55} - \Omega_1^2 & M_{56} \\ (M_{16})^* & (M_{26})^* & (M_{36})^* & (M_{46})^* & (M_{56})^* & M_{66} - \Omega_1^2 \end{pmatrix}, \tag{12}$$

where the elements of the dynamical matrix for the first neighboring spring are

$$\begin{aligned} M_{11} &= \sum_{i=1}^3 3u_i^2 s_{iz}^2, & M_{12} &= \sum_{i=1}^3 -3u_i^2 s_{iz} c_{iz}, & M_{13} &= \sum_{i=1}^3 -\sqrt{3}u_i v_i s_{iz}, \\ M_{14} &= \sum_{i=1}^3 3u_i^2 s_{iz}^2 e^{i\beta_i}, & M_{15} &= \sum_{i=1}^3 3u_i^2 s_{iz} c_{iz} e^{i\beta_i}, & M_{16} &= \sum_{i=1}^3 \sqrt{3}u_i v_i s_{iz} e^{i\beta_i}, \\ M_{22} &= \sum_{i=1}^3 3u_i^2 c_{iz}^2, & M_{23} &= \sum_{i=1}^3 \sqrt{3}u_i v_i c_{iz}, & M_{24} &= \sum_{i=1}^3 -3u_i^2 s_{iz} c_{iz} e^{i\beta_i}, \\ M_{25} &= \sum_{i=1}^3 -3u_i^2 c_{iz}^2 e^{i\beta_i}, & M_{26} &= \sum_{i=1}^3 -\sqrt{3}u_i v_i c_{iz} e^{i\beta_i}, & M_{33} &= \sum_{i=1}^3 v_i^2, \\ M_{34} &= \sum_{i=1}^3 -\sqrt{3}u_i v_i s_{iz} e^{i\beta_i}, & M_{35} &= \sum_{i=1}^3 -\sqrt{3}u_i v_i c_{iz} e^{i\beta_i}, & M_{36} &= \sum_{i=1}^3 -v_i^2 e^{i\beta_i}, \\ M_{44} &= \sum_{i=1}^3 3u_i^2 s_{iz}^2, & M_{45} &= \sum_{i=1}^3 3u_i^2 s_{iz} c_{iz}, & M_{46} &= \sum_{i=1}^3 \sqrt{3}u_i v_i s_{iz}, \\ M_{55} &= \sum_{i=1}^3 3u_i^2 c_{iz}^2, & M_{56} &= \sum_{i=1}^3 \sqrt{3}u_i v_i c_{iz}, & M_{66} &= \sum_{i=1}^3 -v_i^2, \end{aligned}$$

where  $s_{iz} \equiv \sin(\frac{u_i \theta_z}{2})$ ,  $c_{iz} \equiv \cos(\frac{u_i \theta_z}{2})$  and  $\beta_i \equiv qav_i + \alpha u_i \theta_z$ . The dimensionless quantity  $\Omega_1^2$  is defined as  $M\omega^2/K_1$ ,  $K_1$  is the force constant for first neighboring spring.

For  $A$  atom with coordinate  $R_A$ , its six second neighbors are at,

$$R_A^{(1,2,3)} = [R \cos(\theta_{tl} + v_i \theta_z), R \sin(\theta_{tl} + v_i \theta_z), \bar{l}c + 3au_i], \quad i = 1, 2, 3 \tag{13}$$

$$R_A^{(4,5,6)} = [R \cos(\theta_{tl} - v_i \theta_z), R \sin(\theta_{tl} - v_i \theta_z), \bar{l}c - 3au_i], \quad i = 1, 2, 3. \tag{14}$$

The unit vectors to them are

$$\begin{aligned} \tilde{\delta}^{(i)} &= \left[ -v_i \sin\left(\theta_{tl} + \frac{v_i}{2}\theta_z\right), u_i \cos\left(\theta_{tl} + \frac{u_i}{2}\theta_z\right), \sqrt{3}u_i \right], \quad i = 1, 2, 3 \\ \tilde{\delta}^{(i+3)} &= -\tilde{\delta}^{(i)}, \quad i = 1, 2, 3. \end{aligned} \tag{15}$$

To spring between the second neighbors, the potential term for *A* sublattice has six parts:

$$\begin{aligned} \tilde{\Xi}^{(i)} &= e^{i3qau_i + i\alpha v_i \theta_z} \left[ v_i \sin\left(\frac{v_i \theta_z}{2}\right) Q_{A,\rho} + v_i \cos\left(\frac{v_i \theta_z}{2}\right) Q_{A\theta} + \sqrt{3}u_i Q_{Az} \right] \\ &\quad + v_i \sin\left(\frac{v_i \theta_z}{2}\right) Q_{A\rho} - v_i \cos\left(\frac{v_i \theta_z}{2}\right) Q_{A\theta} - \sqrt{3}u_i Q_{Az}, \quad i = 1, 2, 3 \\ \tilde{\Xi}^{(i+3)} &= e^{-i3qau_i - i\alpha v_i \theta_z} \left[ v_i \sin\left(\frac{v_i \theta_z}{2}\right) Q_{A,\rho} - v_i \cos\left(\frac{v_i \theta_z}{2}\right) Q_{A\theta} - \sqrt{3}u_i Q_{Az} \right] \\ &\quad + v_i \sin\left(\frac{v_i \theta_z}{2}\right) Q_{A\rho} + v_i \cos\left(\frac{v_i \theta_z}{2}\right) Q_{A\theta} + \sqrt{3}u_i Q_{Az}, \quad i = 1, 2, 3. \end{aligned} \tag{16}$$

They can be reduced to

$$\begin{aligned} \tilde{\Xi}^{(i)} &= 2e^{i\tilde{\beta}_i/2} \left\{ v_i \sin\left(\frac{v_i \theta_z}{2}\right) Q_{A,\rho} \cos\tilde{\beta}_i/2 \right. \\ &\quad \left. + i \left[ v_i \cos\left(\frac{v_i \theta_z}{2}\right) Q_{A\theta} + \sqrt{3}u_i Q_{Az} \right] \sin(\tilde{\beta}_i/2) \right\}, \quad i = 1, 2, 3, \\ \tilde{\Xi}^{(i+3)} &= (\tilde{\Xi}^{(i)})^*, \quad i = 1, 2, 3, \end{aligned} \tag{17}$$

where  $\tilde{\beta}_i = 3qau_i + \alpha\theta_z v_i$ ,  $z^*$  denotes the complex conjugate of  $z$ . Obviously,  $|\tilde{\Xi}^{(i+3)}| = |\tilde{\Xi}^{(i)}|$ . The dynamical matrix for the oscillation of the *A* sublattice is

$$0 = \det \begin{vmatrix} 8 \sum_{i=1}^3 v_i^2 \tilde{s}_{iz}^2 C_i^2 - \Omega_2^2 & 8 \sum_{i=1}^3 i v_i^2 \tilde{s}_{iz} \tilde{c}_{iz} S_i C_i & 8 \sum_{i=1}^3 i \sqrt{3} u_i v_i \tilde{s}_{iz} S_i C_i \\ -8 \sum_{i=1}^3 i v_i^2 \tilde{s}_{iz} \tilde{c}_{iz} S_i C_i & 8 \sum_{i=1}^3 v_i^2 \tilde{c}_{iz}^2 S_i^2 - \Omega_2^2 & 8 \sum_{i=1}^3 \sqrt{3} u_i v_i \tilde{c}_{iz} S_i^2 \\ -8 \sum_{i=1}^3 i \sqrt{3} u_i v_i \tilde{s}_{iz} S_i C_i & 8 \sum_{i=1}^3 \sqrt{3} u_i v_i \tilde{c}_{iz} S_i^2 & 8 \sum_{i=1}^3 3u_i^2 S_i^2 - \Omega_2^2 \end{vmatrix}, \tag{18}$$

where  $\tilde{s}_{iz} \equiv \sin(\frac{v_i \theta_z}{2})$ ,  $\tilde{c}_{iz} \equiv \cos(\frac{v_i \theta_z}{2})$ ,  $S_i \equiv \sin(\frac{\tilde{\beta}_i}{2})$ , and  $C_i \equiv \cos(\frac{\tilde{\beta}_i}{2})$ . The dimensionless quantity  $\Omega_2^2 \equiv M\omega^2/K_2$ .  $K_2$  is the spring constant for the second neighboring spring.

For a sheet of graphite, the vibrations perpendicular to the plane are well described by bond-bending forces. For SWNTs, radial bond bending is reflected as<sup>7</sup>

$$V_3 = \frac{K_3}{2} \sum_j |\Delta_j|^2, \tag{19}$$

$$|\Delta_j| = \sum_{i=1}^3 \hat{n}_i \cdot (\mathbf{Q}_j^{(i)} - \mathbf{Q}_j), \tag{20}$$

where  $\mathbf{Q}_j^{(i)}$  are the first neighbors of  $\mathbf{Q}_j$ .

If  $\mathbf{Q}_j$  denotes an *A* atom, the normal vectors are

$$\mathbf{n}_i = \left[ \cos \left( \theta_{tl} + \frac{u_i}{2} \theta_z \right), \sin \left( \theta_{tl} + \frac{u_i}{2} \theta_z \right), 0 \right], \quad i = 1, 2, 3. \tag{21}$$

$$\begin{aligned} \Delta_A = e^{iqav_i + i\alpha u_i \theta_z} & \left[ Q_{B\rho} \cos \left( \frac{u_i \theta_z}{2} \right) - Q_{B\theta} \sin \left( \frac{u_i \theta_z}{2} \right) \right], \\ & - \left[ Q_{A\rho} \cos \left( \frac{u_i \theta_z}{2} \right) + Q_{A\theta} \sin \left( \frac{u_i \theta_z}{2} \right) \right] \end{aligned} \tag{22}$$

$$\begin{aligned} \Delta_B = e^{-iqav_i - i\alpha u_i \theta_z} & \left[ Q_{A\rho} \cos \left( \frac{u_i \theta_z}{2} \right) + Q_{A\theta} \sin \left( \frac{u_i \theta_z}{2} \right) \right] \\ & - \left[ Q_{B\rho} \cos \left( \frac{u_i \theta_z}{2} \right) - Q_{B\theta} \sin \left( \frac{u_i \theta_z}{2} \right) \right]. \end{aligned} \tag{23}$$

The phonon potential  $V_3$  leads to a dynamical matrix

$$0 = \det \begin{vmatrix} c^2 + |\tilde{c}|^2 - \Omega_3^2 & cs + \tilde{c}\tilde{s}^* & -2c\tilde{c} & s1\tilde{c} + c\tilde{s} \\ cs + \tilde{s}\tilde{c}^* & s^2 + |\tilde{s}|^2 - \Omega_3^2 & -s\tilde{c} - c\tilde{s} & 2s\tilde{s} \\ -2c\tilde{c}^* & -s\tilde{c}^* - c\tilde{s}^* & c^2 + |\tilde{c}|^2 - \Omega_3^2 & -cs - \tilde{s}\tilde{c}^* \\ s\tilde{c}^* + c\tilde{s}^* & 2s\tilde{s}^* & -cs - \tilde{c}\tilde{s}^* & s^2 + |\tilde{s}|^2 - \Omega_3^2 \end{vmatrix}, \tag{24}$$

where  $c \equiv \sum_{i=1}^3 \cos(\frac{u_i \theta_z}{2})$ ,  $\tilde{c} \equiv \sum_{i=1}^3 \cos(\frac{u_i \theta_z}{2}) e^{i\beta_i}$ ,  $s \equiv \sum_{i=1}^3 \sin(\frac{u_i \theta_z}{2})$  and  $\tilde{s} \equiv \sum_{i=1}^3 \sin(\frac{u_i \theta_z}{2}) e^{i\beta_i}$ . The dimensionless quantity  $\Omega_3^2 = M\omega^2/2K_3$ .  $K_3$  is the spring constant for radial bond bending.

We add together all three interactions with the weights  $r_1 = 1$ ,  $r_2 = K_2/K_1$  and  $r_3 = K_3/K_1$ , and get six equations:

$$\begin{aligned} \Omega_1^2 Q_{A\rho} = & \left[ \left( \sum_{i=1}^3 3u_i^2 s_{iz}^2 \right) Q_{A\rho} + \dots \right] + r_2 \left[ \left( 8 \sum_{i=1}^3 v_i^2 \tilde{s}_{iz}^2 C_i^2 \right) Q_{A\rho} + \dots \right] \\ & + r_3 \left[ \left( c^2 + |\tilde{c}|^2 \right) Q_{A\rho} + \dots \right], \quad \text{etc.}, \end{aligned}$$

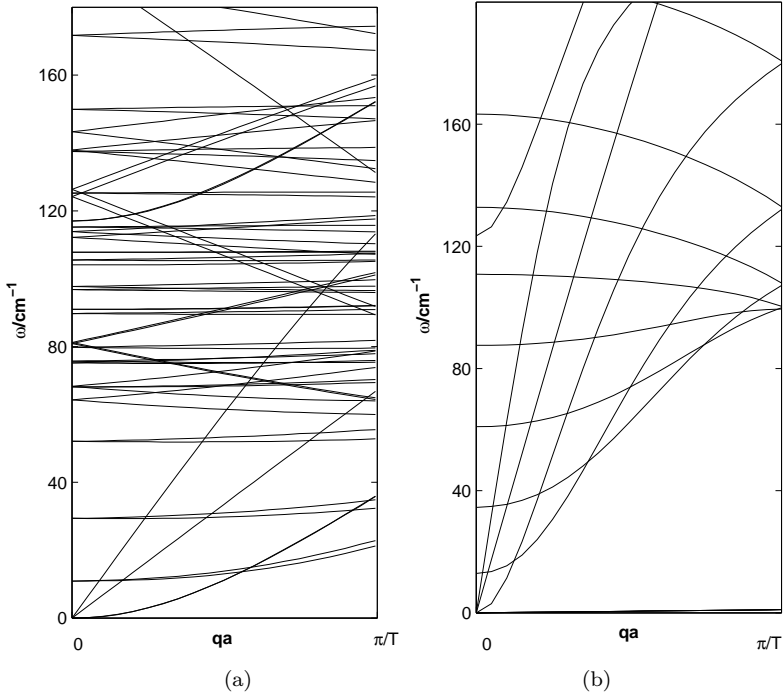


Fig. 2. (a) Phonons dispersion relation was shown for half of the first Brillouin zone for a zigzag (10, 0) tube.  $\alpha = 0, 1, 2, \dots, N - 1$ . The definition of  $\alpha$  is in the text. Flexure mode is twofold degenerate. (b) Large scale presentation of the region at low frequency of (10, 0) SWNT.

which give the physical results. There are two acoustical modes at  $\alpha = 0$ , i.e., longitudinal acoustical phonon and twist mode.  $\alpha = 1, N - 1$  each gives one flexure mode. When  $\alpha = 0$ , the solutions of the above equations have ZO modes (similar to out-of-plane optical phonon mode for a sheet of graphene). Velocities of the sound,  $v_L$  and  $v_{TW}$  estimated from the density and Young’s modulus of SWNT, and  $\omega_{ZO}$  are important for fitting force constants.<sup>1</sup>

From these equations, we can calculate the correct phonon dispersion of SWNTs. To manifest the efficiency of our method, we calculate a zigzag SWNT (10, 0) and a chiral one (10, 1), (see Figs. 2 and 3), and compare their phonon dispersion relations. Similar to Ref. 7, we set  $\Omega_1 = \sqrt{3}$  to the optical phonon at  $1600 \text{ cm}^{-1}$ ,  $r_2 = 0.06, r_3 = 0.024$ . For (10, 0) SWNT, the two acoustic modes have velocities  $v_L = 16.4 \text{ km/s}$  and  $v_{TW} = 8.7 \text{ km/s}$ . The optical phonons are at frequencies  $291 \text{ cm}^{-1}, 877 \text{ cm}^{-1}, 1580 \text{ cm}^{-1}$  and  $1600 \text{ cm}^{-1}$ . The flexure modes occur at  $\alpha = 1$  and  $\alpha = 19$ . For (10, 1) SWNT, the two acoustic modes have velocities  $v_L = 16.5 \text{ km/s}$  and  $v_{TW} = 8.2 \text{ km/s}$ . The optical phonons are at frequencies  $277 \text{ cm}^{-1}, 875 \text{ cm}^{-1}, 1582 \text{ cm}^{-1}$  and  $1605 \text{ cm}^{-1}$ . The flexure modes occur at  $\alpha = 1$  and  $\alpha = 73$ . Therefore, the long wavelength modes of low frequency have two acoustic modes and two flexure modes for both achiral SWNTs and and chiral



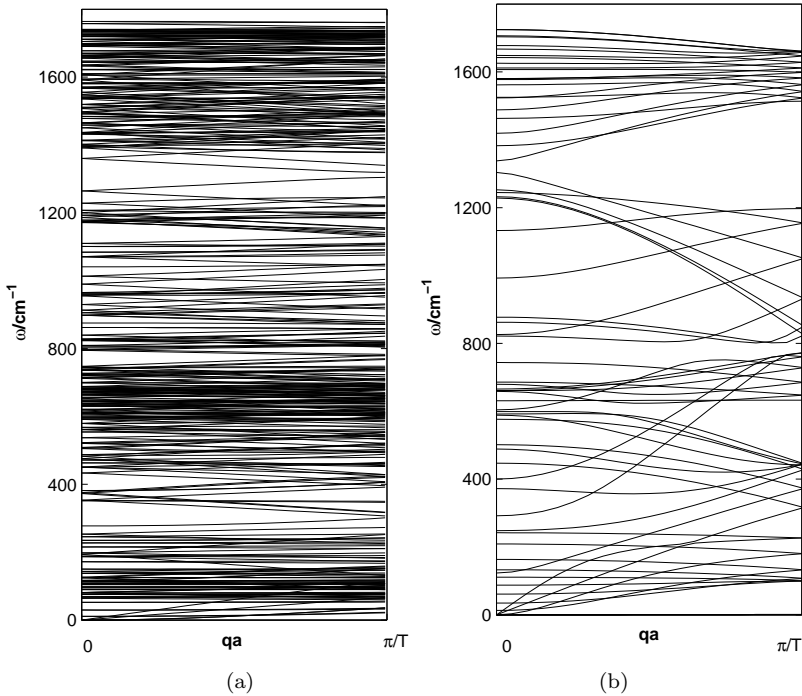


Fig. 3. (a) Phonons dispersion relation was shown for half of the first Brillouin zone for a chiral (10, 1) SWNT.  $\alpha = 0, 1, 2, \dots, N - 1$ . Flexure mode is twofold degenerate. (b) Large scale presentation of the region at low frequency of (10, 1) SWNT.

ones. Mahan obtained this result by elasticity theory. He showed that the results are independent of chirality due to the in-plane isotropic nature of sound waves in the tube.<sup>12</sup> The phonon dispersion relation obtained by the present method has been applied to study chirality dependence of the radial breathing phonon mode density in zigzag, armchair, and chiral SWNTs, and the influence of the phonon mode density for two phonon resonant Raman scattering problem.<sup>22</sup> We use the minimum number of the force constants that give a physical result (vanishing frequencies of acoustical and flexure phonons at the  $\Gamma$  point). In the present work, we clearly write out all the matrix elements of the six-by-six dynamic matrix in Mahan and Jeon's model. Theoretically, it is not difficult to extend our method to the models with more nearest neighbors taken into account. This work is in progress. In addition, we plan to investigate how the increased number of nearest neighbors affects the results.

In summary, we developed a computational method to calculate the phonon dispersion relation of SWNTs with arbitrary chirality, and obtained reasonable results. In contrast to the chiral SWNTs, the chiral ones with similar radius to them have more phonon modes due to the the larger number of carbon atoms in one translational unit cell for chiral SWNTs. From the phonon dispersion, we can do further research on the phonons-involved phenomena.

## Acknowledgments

We are grateful to Prof. G. D. Mahan for his suggestion of doing research on phonon dispersion relation of chiral nanotubes, and Dr. G. S. Jeon for helpful discussion.

## References

1. R. Saito, G. Dresselhaus and M. S. Dresselhaus, *Physical Properties of Carbon Nanotubes* (Imperial College Press, London, 1998).
2. B. J. LeRoy, S. G. Lemay, J. Kong and C. Dekker, *Nature (London)* **432** (2004) 371.
3. L.-H. Ye, B.-G. Liu, D.-S. Wang and R. Han, *Phys. Rev. B* **69** (2004) 235409.
4. V. N. Popov, V. E. Van Doren and M. Balkanski, *Phys. Rev. B* **59** (1999) 8355.
5. V. N. Popov, V. E. Van Doren and M. Balkanski, *Phys. Rev. B* **61** (2000) 3078.
6. Z. M. Li, V. N. Popov and Z. K. Tang, *Solid State Commun.* **130** (2004) 657.
7. G. D. Mahan and G. S. Jeon, *Phys. Rev. B* **70** (2004) 075405.
8. E. Dobardžić, I. Milošević, B. Nikolić, T. Vuković and M. Damnjanović, *Phys. Rev. B* **68** (2003) 045408.
9. D. Sánchez-Portal, E. Artacho, J. M. Soler, A. Rubio and P. Ordejón, *Phys. Rev. B* **59** (1999) 12678.
10. O. Dubay and G. Kresse, *Phys. Rev. B* **67** (2003) 035401.
11. J.-W. Jiang, H. Tang, B.-S. Wang and Z.-B. Su, *Phys. Rev. B* **73** (2006) 235434.
12. G. D. Mahan, *Phys. Rev. B* **65** (2002) 235402.
13. I. Milošević, E. Dobardžić and M. Damnjanovic, *Phys. Rev. B* **72** (2005) 085426.
14. C. Y. Wang, C. Q. Ru and A. Mioduchowski, *Phys. Rev. B* **72** (2005) 075414.
15. S. V. Goupalov, *Phys. Rev. B* **71** (2005) 085420.
16. K.-P. Bohnen, R. Heid, H. J. Liu, and C. T. Chan, e-print: cond-mat/04111515.
17. L. M. Woods and G. D. Mahan, *Phys. Rev. B* **61** (2000) 10651.
18. M. A. Strocio and M. Dutta, *Phonons in Nanostructures* (Cambridge University Press, Cambridge, 2001).
19. G. D. Mahan, *Phys. Rev. B* **68** (2003) 125409.
20. Z. C. Tu and Z. C. Ou-Yang, *J. Phys. C* **15** (2003) 6759; *Phys. Rev. B* **68** (2003) 153403.
21. M. S. Dresselhaus and P. C. Eklund, *Adv. Phys.* **49** (2000) 705.
22. A. N. Vamivakas, Y. Yin, A. G. Walsh, M. S. Ünlü, B. B. Goldberg and A. K. Swan, *Phys. Rev. B*, submitted.